

Actuation Dynamics of Polymer Hydrogel in Electric Field

Yoshimi SEIDA

Abstract

The actuation dynamics of the strip hydrogel in electric field was investigated as the function of electric field intensity. The electrolytic cell packed with the spherical hydrogel, which simulated the actuation system of the strip hydrogel, was developed to investigate the actuation dynamics of the strip hydrogel in electric field from viewpoints of the ionic and strain/swelling distributions in the strip hydrogel. The actuation behavior of the strip hydrogel with the characteristic motion/bending pattern depending on the electric field intensity was analyzed based on elastic mechanics of beam bending coupled with osmotic pressure model of the hydrogel, using the ionic and strain/swelling distribution data obtained by the packed bed electrolytic cell system. The bending pattern of strip hydrogel was simulated fairly well by the theoretical model using the swelling data collected by the packed bed system. The actuation mechanism of the gel in electric field was clarified through the series of the study.

Keywords: polymer hydrogel, actuation, Donnan equilibrium, transport phenomena, electric field

1. Introduction

The deformation of ionic polymer hydrogels in an electric field is a well known phenomenon that will enable the gels applicable in many engineering and medical use. Following the discovery of the phenomenon by Tanaka *et al.* in 1982 (Tanaka *et al.*, 1982), a lot of similar phenomena observing actuation of gels have been reported in various polymer films and polymer gels (Osada and Hasebe, 1985; Osada and Okuzaki, 1992; Shiga and Kurauchi, 1990; Shiga *et al.*, 1993; DeRossi *et al.*, 1986). Mechanism of the deformation or the actuation is basically related to transport phenomena of ions in the gel, so has been studied from the viewpoint of transport phenomena of ions and osmotic/swelling pressure of gel that is influenced strongly by ionic distribution. Seida *et al.* has also pointed out that the deformation occurs by a change of osmotic pressure of gel that was induced by ionic transport inside gel (Nakano and Seida, 1995, Seida and Nakano, 1990, 1991, 1995). The osmotic pressure will be caused by the difference in ionic concentration between inside and

outside the gel. The change of osmotic pressure during the deformation process was also predicted by Doi *et al.* based on theoretical studies of ionic distribution at gel-solution interface of ionic hydrogel in electric field (Doi *et al.*, 1992). It is acceptable to consider that the actuation occurs due to the change in ionic distribution accompanied with the osmotic pressure change. There are, however, few experimental reports that support the proposed actuation mechanism in the strip-gel although it is difficult to identify the ionic distribution during actuation in the strip hydrogel. Further study from the viewpoint of the distributions in electric field is required to understand the mechanism of the phenomena by which a guideline for a precise control of the actuation in engineering and medical applications could be supplied.

In this paper, the actuation dynamics of ionic polymer hydrogel in electric field was investigated in terms of ionic and swelling distributions inside the gel. The characteristic actuation behavior of the strip hydrogel depending on the field intensity was analyzed based on strain and moment distributions induced by ionic transport in the gel in electric field using the distribution data. The ionic transport and moment distribution in the gel during the actuation were examined using an originally developed electrolytic cell with five series open-compartments. The behaviors were theoretically analyzed by a simple elastic model.

2. Experimental

2.1 Sample

A. Particles of PAMPS gel

Poly(2-acrylamido-2-methyl propane) sulfonic acid (PAMPS) was used for the ionic polymer hydrogel that is driven in electric field. The particles of the PAMPS gel were prepared by free radical polymerization at 333 K for 4 hr in the presence of 5 mol% of crosslinker; N,N'-methylene-bis-acrylamide, following the procedure reported (Osada and Hasebe, 1985). The synthesized PAMPS gel was crushed into pieces with a diameter below 1 mm. The crushed particles were immersed in a large amount of distilled water for several days to wash away residual chemicals. The washed particles were then immersed in a large amount of 0.01M Na₂SO₄ aqueous solution to replace the counter ions of PAMPS from proton to sodium ion.

B. The strip of PVA-PAMPS gel

Interpenetrate network between Poly(vinyl alcohol) and PAMPS (PVA-PAMPS) was used as the strip hydrogel in the present study. Mechanical strength of pure PAMPS gel was increased by interpenetrating network of neutral PVA polymer. 15 mmol of 2-acrylamide-2-methyl propane sulfonic acid (AMPS), 1.5 mmol of N,N'-methylene-bisacrylamide; crosslinker, 1.8 mmol of ammonium peroxodisulfate; initiator and 1.25 g of PVA

(polymerization degree 2000 and saponification 99.9 %) were dissolved into 30 ml mixture of distilled water and dimethylsulfoxide (DMSO; 15 g). The solution was heated at room temperature after cooling at 258 K for 6 h in a thin-spaced glass cell to produce PVA network first. The AMPS monomers in the PVA network were polymerized at 333 K for 4 h by free radical polymerization. The prepared strip of PVA-PAMPS gel was washed in a large amount of distilled water to wash away residual chemicals and was then kept in a large amount of 0.01 M Na₂SO₄ aqueous solution to replace the counter ions of AMPS with Na⁺ ions.

2.2 Apparatus and experimental procedure

Two types of electrolytic cells were used to investigate the actuation mechanism of the strip hydrogel in electric field. Cell(A) depicted in Fig. 1 was used to evaluate the actuation behavior of the strip hydrogel as a function of electric field intensity. The strip of PVA-PAMPS gel that was swollen in the 0.01 M Na₂SO₄ aqueous solution (10 mm width, 20 mm length and 1mm thickness) was suspended at the center between rod and plate types of Pt-electrodes in the Cell(A) filled with 0.01 M Na₂SO₄ aqueous solution. Time course of bending angle of the strip hydrogel was measured with a video camera after applying DC electric field across the strip hydrogel. The bending angle (θ) of the strip hydrogel was defined as is shown in Fig.1 and was calculated by the following equation.

$$\theta = 2 \tan^{-1} \left(\frac{y_s}{x_s} \right) \quad (1)$$

where x_s and y_s are the position of the free end of the strip on the x_s - y_s coordinate shown in the figure.

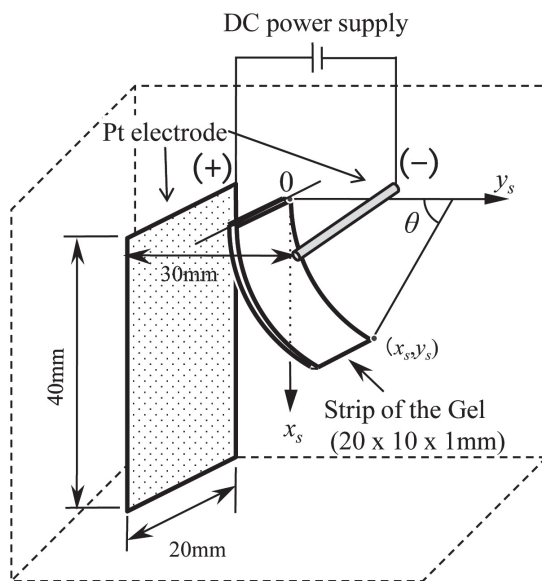


Fig. 1 Electrolytic Cell(A)

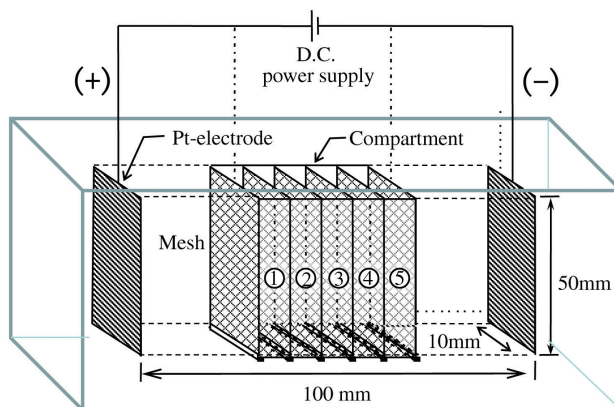


Fig. 2 Electrolytic Cell(B)

Cell(B) depicted in Fig. 2 was used to estimate both ionic and strain/swelling (osmotic pressure) distributions in the strip hydrogel along its thickness during the actuation in electric field. The Cell(B) consists of five open compartments that are separated each other using poly(propylene) mesh sheets. Plate type Pt-electrodes were placed at both sides as shown the layout in Fig. 2. The particles of PAMPS gel swollen in the 0.01M Na_2SO_4 aqueous solution were packed into each compartment uniformly with packing height of 30 mm. The Cell packed with the PAMPS gel was immersed in a bath filled with a large amount of 0.01M Na_2SO_4 aqueous solution. This packed bed simulates the strip hydrogel, thereby the width of 5 compartments (packing beds) corresponds to the thickness of the strip hydrogel. Time courses of both the packing height and the concentration of counter ion in the particles of hydrogel at each compartment were measured after applying dc electric field across the packed bed. The concentration of counter ion in the particles of hydrogel at each compartment was analyzed by means of atomic adsorption spectroscopy after decomposing the hydrogel with 30 wt% H_2O_2 at 363 K following the procedure reported (Seida and Nakano, 1991).

3. Results

The time courses of bending angle of the strip PVA-PAMPS hydrogel are shown in Fig. 3 for the series of electric fields. The strip hydrogel showed characteristic bending pattern depending on the intensity of applied electric field. The strip hydrogel bent slowly toward the anode monotonically up to a saturation angle in the case of small electric field of 1.7 V/cm. On the contrary, a peak of bending angle appeared before reaching a saturation angle that is smaller than the peak angle in the case of large field intensity (> 1.7 V/cm). The initial rate of

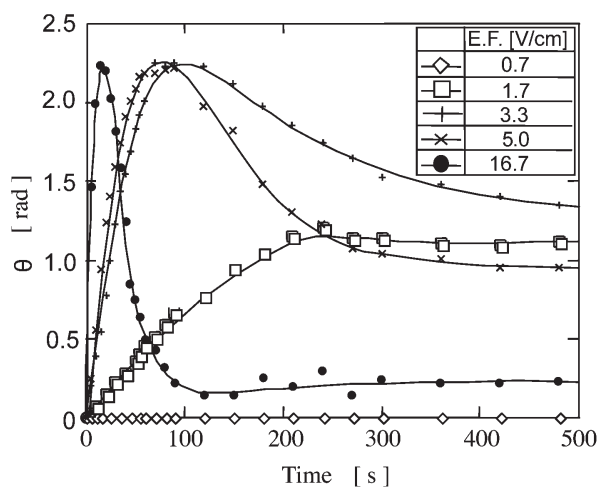


Fig. 3 Actuation behavior of the strip PAMPS-PV gel

bending increased depending on the increase of electric field intensity. When the field intensity was below 1.0 V/cm, the actuation of the strip hydrogel was not induced. Figures 4(a), (b) and (c) show the time course of packing height of the PAMPS gel at each compartment in the Cell(B). The hatched areas in the figures show distribution of packing height width referred to the lowest packing height at each time. The packing height increased with time from cathode

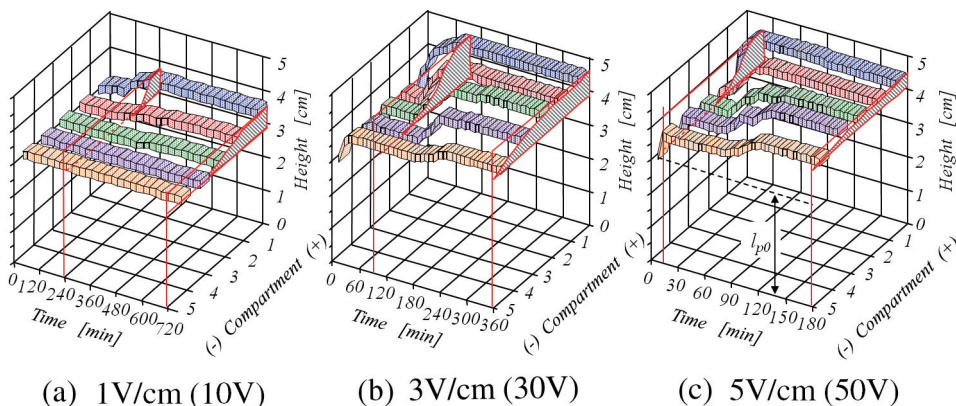


Fig. 4 Time courses of packing heights at each compartment in electrolytic cell(B).

to anode side. The distribution of packing height along the cell width reached a steady state in a few hours. The distribution in the steady state as well as the transient state depended on the applied electric field intensity. The change of packing height prevailed near the anode with increasing the field intensity. Fig. 5 shows the concentration distribution of Na^+ ion; the counter ion, inside the packed gel at each compartment in the Cell(B) (the results in the case of field intensity of 5 V/cm). The concentration of Na^+ ions decreased with time from cathode to anode side.

4. Discussion

The PAMPS gel swelled at the compartment where sodium concentration decreased as can be understood from the results in Figs. 4 and 5. According to Donnan equilibrium analysis of the swelling behavior of ionic polymer hydrogel in electrolyte solution, concentration difference of dominant electrolytes between gel and outer solution determines the osmotic swelling pressure $\Delta\Pi$ working on the gel (Doi *et al.*, 1992; Grimshaw *et al.*, 1990; Omine and Tanaka, 1982). In the present system, Na^+ ion (0.01M) is the

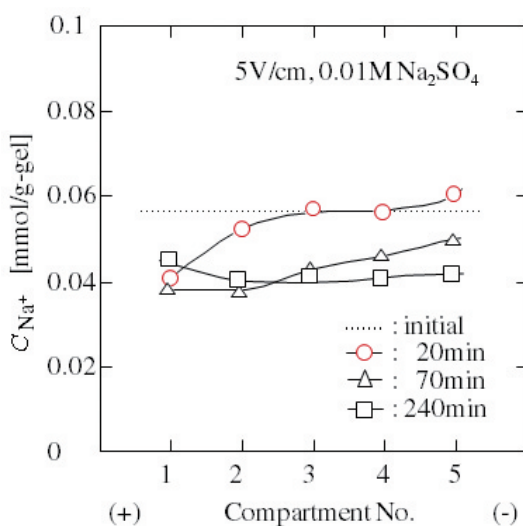


Fig. 5 Concentration distribution of Na^+ in the Cell (B)

dominant ion, thereby the swelling of the PAMPS gel is to be controlled depending on the concentration of Na^+ ion at each compartment in the Cell(B).

The mechanism of bending of the strip hydrogel could be interpreted based on the Donnan equilibrium theory and the elastic mechanics from viewpoint of stress distribution inside the gel. Fig. 6 indicates the dependence of the $\Delta\Pi$ on the concentration of both counter ($C_{A,g}$) and *co*-ions ($C_{B,g}$) inside ionic polymer hydrogel, which was calculated based on the Donnan equilibrium theory (Doi *et al.*, 1992). The decrease of counter ion inside the gel ($C_{A,g}$) results in the increase of $\Delta\Pi$ (Starting point of the arrow in the figure corresponds to the initial condition in the system under study). In the strip system, the concentration of Na^+ ion (the counter ion) will decrease at cathode side of the gel in electric field as was predicted in Fig. 5. The osmotic pressure $\Delta\Pi$ increases followed by swelling of the gel at the region where the $C_{A,g}$ decreases, which results in the bending to anode side in the case of strip hydrogel. The Donnan mechanism in electric field plays the significant role in producing the ionic distribution inside gel. The change in swelling (osmotic pressure of the gel) depending on the ionic concentration inside the hydrogel is the key mechanism of the bending.

The packing height in the packed bed system (the Cell(B)) corresponds to the swelling volume (osmotic pressure) in the strip hydrogel along its thickness under a condition free from its internal stress restriction. Elastic theory of beam bending was applied to interpret the bending pattern of strip hydrogel (Timoshenko and Young, 1968; Tamate and Abe, 1978). Suppose a strip hydrogel which bends depending on its internal stress distribution along its thickness (Fig. 7(a)). The bending angle of the strip defined in Fig.1 can be determined by the balance of both force and moment working on the strip. According to Hooke's law

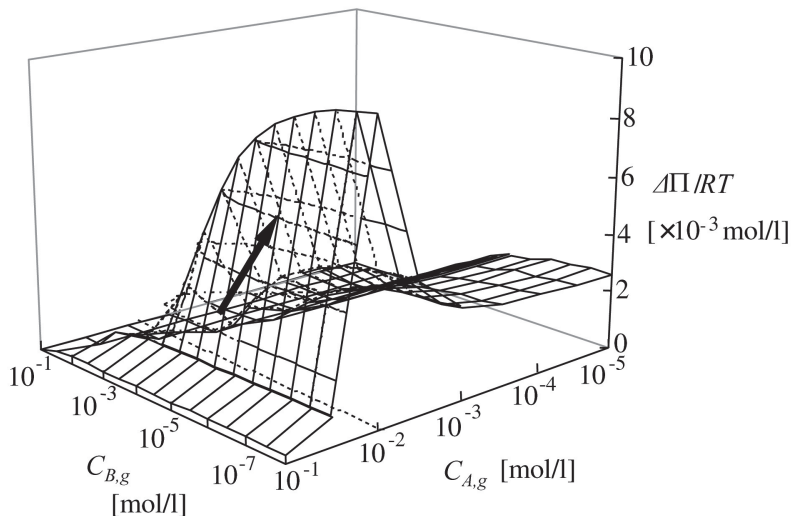


Fig. 6 Bird's eye view of ($C_{A,g}$, $C_{B,g}$) dependent of $\Delta\Pi$ for the system of $K_g=1 \times 10^3$ mol/l and $C_M=10^2$ mol/l. $A=\text{Na}^+$, $B=\text{SO}_4^{2-}$

($\sigma = E\varepsilon$), the strain, ε , at each point along thickness direction of the strip is given by Eq. (2).

$$\varepsilon_{s,x} = \frac{(l_{s,x} - l'_{s,x})}{l'_{s,x}} \quad (2)$$

where $l_{s,x}$ and $l'_{s,x}$ are the length of strip at position x in the strip under mechanically balanced steady state and the length in state free from internal stress restriction along the thickness of strip, respectively. The stress and the moment working on the strip should be balanced simultaneously as a whole to satisfy the following Eqs. (3) and (4) based on elastic mechanics.

$$\begin{aligned} \int_{x=0}^{x=d_s} \sigma_x dx &= \int_{x=0}^{x=d_s} E \varepsilon_{s,x} dx = \int_{x=0}^{x=d_s} E \frac{(l_{s,x} - l'_{s,x})}{l'_{s,x}} dx \\ &= \int_{x=0}^{x=d_s} E \frac{((x+a)\theta - l'_{s,x})}{l'_{s,x}} dx = 0 \end{aligned} \quad (3)$$

$$\begin{aligned} \int_{x=0}^{x=d_s} \sigma_x (x+a) dx &= \int_{x=0}^{x=d_s} E \varepsilon_{s,x} (x+a) dx = \int_{x=0}^{x=d_s} E \frac{(l_{s,x} - l'_{s,x})}{l'_{s,x}} (x+a) dx \\ &= \int_{x=0}^{x=d_s} E \frac{((x+a)\theta - l'_{s,x})}{l'_{s,x}} (x+a) dx = 0 \end{aligned} \quad (4)$$

where $x+a$ and E are the radius of curvature of the bending and Young's modulus, respectively. Eqs. (3) and (4) can be expressed by Eqs.(5) and (6) respectively in discrete form. The packing height data in the packed bed system that corresponds to the length in state free from internal stress restriction in the case of strip can be applied.

$$\sum_{i=1}^N \frac{(\Delta d_p (i - \frac{1}{2}) + a) \theta - l'_{p,i}}{l'_{p,i}} = 0 \quad \left(\Delta d_p = \frac{d_p}{N} \right) \quad (5)$$

$$\sum_{i=1}^N \frac{(\Delta d_p (i - \frac{1}{2}) + a) \theta - l'_{p,i}}{l'_{p,i}} (\Delta d_p (i - \frac{1}{2}) + a) = 0 \quad (6)$$

The bending angle θ of the strip will be estimated by Eq. (7) using only the packing height data, $l'_{p,i}$ that is observable in the packed bed system

$$\theta = \frac{\left(\frac{d_p}{2} A - B\right) DN}{AC - B^2} \quad (N = 5) \quad (7)$$

where

$$\begin{aligned} A &= \sum_{j=1}^N \left[\left(\prod_{i=1}^N l'_{p,i} \right) / l'_{p,j} \right], B = \sum_{j=1}^N \left[\left(\prod_{i=1}^N l'_{p,i} \right) (\Delta d_p (j - \frac{1}{2})) / l'_{p,j} \right] \\ C &= \sum_{j=1}^N \left[\left(\prod_{i=1}^N l'_{p,i} \right) (\Delta d_p (j - \frac{1}{2}))^2 / l'_{p,j} \right], D = \prod_{i=1}^N l'_{p,i} \end{aligned}$$

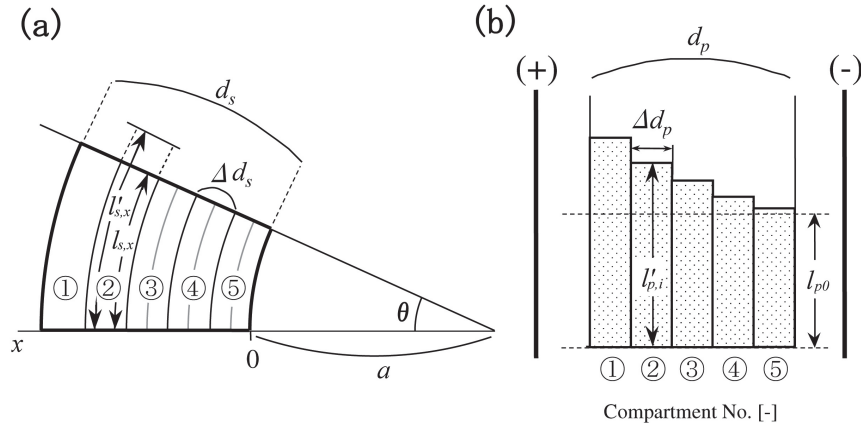


Fig. 7 Correlation diagram between the strip hydrogel and the packed bed system

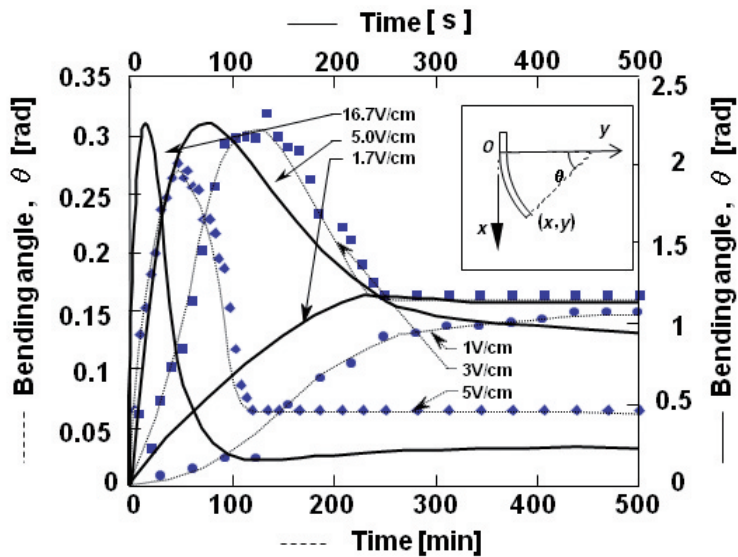


Fig. 8 Simulated bending behavior.

Fig. 8 shows time courses of bending angle θ simulated by Eq.(7) using the results in Fig. 4. In the small field intensity (1 V/cm), the bending angle increased monotonically up to a steady state one. On the contrary, the bending showed a maximum value/peak and turned back to a steady state angle in the case of strong field intensity (3, 5 V/cm). Even though the results in Figs. 3 and 8 are different each other in both time scale and magnitude of bending angle due to the difference in the size of sample between the packed bed and the strip, the simulated time course of bending corresponds to the bending behavior of the strip PVA-PAMPS gel fairly well in its trend. When the change of strain distribution occurs beyond the center of the strip (Figs. 4(b) and (c)), the peak of bending with a steady state bending angle

appears.

From these results, it was found that the bending behavior of strip of ionic polymer hydrogel depends on ionic distribution along its thickness. The production of the ionic distribution is the specific phenomenon observed in ionic hydrogel that is placed in electric field (the “ionic” means the gel contains immobilized ionic group). The distribution pattern depends on the strength of electric field, thus the specific bending pattern appears as a function of the electric field.

5. Conclusion

The dynamics of bending behavior of ionic polymer hydrogel in an electric field was investigated theoretically as well as experimentally in terms of ionic and swelling distributions inside the gel. The bending behavior of the gel depends on its internal swelling (stress) distribution that is induced depending on the ionic distribution inside the gel. The bending behaviors were simulated fairly well as a function of electric field based on the theoretical elastic model.

Acknowledgement

The author acknowledges to Mr. Ohno for his experimental assistance and Emeritus Prof. Y. Nakano for his valuable discussion.

Nomenclature

a :	radius of the bending
C :	concentration
d :	thickness of the media
K_g :	Donnan ratio
l :	length
N :	the number of compartment
x :	position on the x-y coordinate
y :	position on the x-y coordinate
ε :	strain
σ :	stress
$\Delta\Pi$:	osmotic pressure

Suffix

i :	compartment No.
-------	-----------------

<i>M</i> :	ionic group in the gel
<i>p</i> :	packed bed system
<i>s</i> :	strip system
' :	state free from stress
0:	initial condition

References

- DeRossi, D. E., Chiarelli, P., Buzzigoli, G., Domenici, C. and Lazzeri, L., Contractile behavior of electrically activated mechanochemical polymer actuators, *Am. Soc. Artif. Intern Organs*, **32**, 157-162(1986)
- Doi, M., Matsumoto, M. and Hirose, Y., Deformation of ionic polymer gels by electric fields, *Macromolecules*, **25**, 5504-5511(1992)
- Grimshaw, P. E., Nussbaum, J.H. and Grodzinsky, A. J., Kinetics of electrically and chemically induced swelling in polyelectrolyte gels, *J. Chem. Phys.*, **93**(6), 4462-4472 (1990)
- Nakano, Y. and Seida, Y., Solvent release in polymer hydrogel by electrochemical method, *Kagakukogaku Ronbunshu*, **21**(2), 321-326(1995)
- Omine, I. and Tanaka, T., Salt effects on the phase transition of ionic gels, *J. Chem. Phys.*, **77**(11), 5725-5729(1982)
- Osada, Y. and Hasebe, M., Electrically activated mechanochemical devices using polyelectrolyte gels, *Chem. Lett.*, 1285-1288(1985).
- Osada, Y. and Okuzaki, H., A polymer gel with electrically driven motility, *Nature*, **355**(16), 242-244(1992)
- Seida, Y. and Nakano, Y., Shrinking behavior and dehydration of ionic hydrogel in an electric field, *Kagakukogaku Ronbunshu*, **16**(6), 1279-1282(1990)
- Seida, Y. and Nakano, Y., Transport of ions inside polymer gel in an electric field, *J. Chem. Eng. Japan*, **24**(6), 755-760(1991)
- Seida, Y. and Nakano, Y., Concept to control the phase behavior of stimuli-sensitive polymer gel, *J. Chem. Eng. Japan*, **28**(4), 425-428(1995)
- Shiga, T. and Kurauchi, T., Deformation of polyelectrolyte gels under the influence of electric field, *J. Applied Polymer Science*, **39**, 2305-2320(1990)
- Shiga, T., Hirose, Y., Okada, A. and Kurauchi, T., Electrically driven polymer gel finger working in the air, *J. Intelligent material systems and structures*, **4**, 553-557(1993)
- Tamate, O. and Abe, H., *Zairyou rikigaku, Morikita Syuppan*, Tokyo, 1(1978)
- Tanaka, T., Nishio, I., Sun, S. T. & Ueno-Nishino, S., Collapse of gels in an electric field, *Science*, **218** (4571), 467-469(1982).
- Timoshenko, S. P. and Young, D. H., *Elements of strength of materials, 5th ed.*, Maruzen, Tokyo, Japan(1968)

Appendix

From Eqs. (5) and (6), following equations (a1) and (a2) are derived.

$$\theta \left(\frac{\Delta d_p \left(1 - \frac{1}{2}\right) + a}{l'_{p,1}} + \frac{\Delta d_p \left(2 - \frac{1}{2}\right) + a}{l'_{p,2}} + \dots + \frac{\Delta d_p \left(N - \frac{1}{2}\right) + a}{l'_{p,N}} \right) - N = 0 \quad (\text{a1})$$

$$\begin{aligned} & \theta \left(\frac{\left(\Delta d_p \left(1 - \frac{1}{2}\right) + a\right)^2}{l'_{p,1}} + \frac{\left(\Delta d_p \left(2 - \frac{1}{2}\right) + a\right)^2}{l'_{p,2}} + \dots + \frac{\left(\Delta d_p \left(N - \frac{1}{2}\right) + a\right)^2}{l'_{p,N}} \right) \\ & - \sum_{i=1}^N \left(\Delta d_p \left(i - \frac{1}{2}\right) + a \right) \\ & = \left(\frac{\left(\Delta d_p \left(1 - \frac{1}{2}\right) + a\right)^2}{l'_{p,1}} + \frac{\left(\Delta d_p \left(2 - \frac{1}{2}\right) + a\right)^2}{l'_{p,2}} + \dots + \frac{\left(\Delta d_p \left(N - \frac{1}{2}\right) + a\right)^2}{l'_{p,N}} \right) \\ & - \left(\Delta d_p \frac{N(N+1)}{2} - \frac{1}{2} \Delta d_p N + aN \right) = 0 \quad (\text{a2}) \end{aligned}$$

Eqs.(a1) and (a2) respectively are expressed using the summarized parameters, A , B , C and D shown in the main text as follows.

$$Aa\theta + B\theta - DN = 0 \quad (\text{a3})$$

$$Aa^2\theta + 2Ba\theta + C\theta - D \left(\frac{d_p}{2} + a \right) N = 0 \quad (\text{a4})$$

From Eq.(a3), Eq.(a5) was derived and the Eq.(a5) was introduced into Eq.(a4), resulting in Eq.(7).

$$a = \frac{DN - B\theta}{A\theta} \quad (\text{a5})$$

要 旨

イオン性ハイドロゲルの電場における運動動力学

清田佳美

高分子ハイドロゲル膜が電場において自律的に運動する現象の動力学の解明を試みた。運動過程におけるゲル内の物質移動ならびにゲルに発生する浸透圧を明らかにする目的で、区切られた複数のオープンコンパートメントを有するゲル粒子充填電解セルを新たに開発した。このセルを用いて電場におけるゲル内のイオン分布の経時変化、発生応力およ

び発生歪み分布の経時変化を観察した。ゲルの運動を誘発するメカニズムとして、イオンの分布形成に基づくゲルの浸透圧分布の形成とこれに伴う応力（ひずみ）分布の形成を仮定し、弾性力学に基づくゲル膜の運動モデルを構築した。このモデルとゲル粒子充填型電解セルで得られたデータを用いて、印加する電場の強さに依存してゲル膜の運動パターンが特異的に変化する様子を定性的に再現することができた。ゲルの運動現象は、ゲルに発生する浸透圧分布に依存してその運動パターンが特異的に変わることを確認した。